Aerosol Science and Technology

ISSN: 0278-6826 (Print) 1521-7388 (Online) Journal homepage: http://www.tandfonline.com/loi/uast20

Removal Rates of Explosive Particles From a Surface by Impingement of a Gas Jet

Ryan Keedy , Evan Dengler , Peter Ariessohn , Igor Novosselov & Alberto Aliseda

To cite this article: Ryan Keedy , Evan Dengler , Peter Ariessohn , Igor Novosselov & Alberto Aliseda (2012) Removal Rates of Explosive Particles From a Surface by Impingement of a Gas Jet, Aerosol Science and Technology, 46:2, 148-155, DOI: 10.1080/02786826.2011.616920

To link to this article: http://dx.doi.org/10.1080/02786826.2011.616920

Accepted author version posted online: 26 Aug 2011.

Aerosol Science and Technology, 46:148–155, 2012

ISSN: 0278-6826 print / 1521-7388 online
DOI: 10.1080/02786826.2011.616920

Removal Rates of Explosive Particles From a Surface by Impingement of a Gas Jet

Ryan Keedy,[1] Evan Dengler,[2] Peter Ariessohn,[2] Igor Novosselov,[2] and Alberto Aliseda[1]

[1]*Mechanical Engineering Department, University of Washington, Seattle, Washington, USA*
[2]*Enertechnix, Inc., Maple Valley, Washington, USA*

The rate of particle removal from a surface by air jet impingement has been evaluated for 3 different types of trace explosives. Samples of research development explosive (cyclotrimethylenetrinitramine), trinitrotoluene, and C-4 were each transferred to glass surfaces and then subjected to a short burst of air from a jet with varying diameter, standoff distance, and backpressure to achieve a range of shear stresses at the surface. TNT was observed to be easiest to remove, while C-4 required the greatest shear force to resuspend. An analytical model has been developed to predict removal of spherical particles as a function of particle diameter and nondimensionalized downstream distance from a gas jet. This model was fitted to experimental data from the removal of ceramic microspheres of various sizes. The removal rate of these ceramic microspheres was observed to be much greater than that of the 3 types of explosive particles, despite the particles' similar sizes.

INTRODUCTION

The removal of small solid particles from solid surfaces is a ubiquitous problem in material processing. While most of these applications rely on liquid solvents to extract the solid residue from a process surface, there are many cases in which a nonintrusive clean up process is preferable to reduce cost and limit the possible damage or contamination of the surface.

In addition, there is a need for noninvasive sampling and inspection of contaminating residues that may indicate chemical, radiological, or biological hazards. Fine particulates of explosives may be dislodged during the bomb making or handling process and may adhere to available surfaces. Bender et al. (1992) observed that low volatility explosive vapors tend to adsorb onto surfaces or dust particles that may settle on a surface. Davidson and Scott (2002) noted that this presents an opportunity for several explosive detection schemes based on particulate sampling. A recommendation of the recently released report of the National Research Council on Existing and Potential Standoff Explosives Detection Techniques calls for "the use of convective streams with or without airborne adsorbing particles to gather chemical samples" (National Research Council 2004). This advocates the approach of dislodging molecular vapors and particles containing traces of explosives from the surface and near-surface boundary layer by increasing convective mass transfer, which would allow them to be captured and analyzed.

Particle removal depends on particle, surface, and jet properties. A high-speed gas jet impinging on a solid surface drives a tangential flow with a thin boundary layer, thereby producing high shear stresses on the surface. This exerts a force on the particles that can potentially overcome the adhesive forces binding the particles to the surface as well as their own weight, and suspend them in the gas stream. The gas stream can then be sampled by a detector designed to collect and analyze the suspended particles.

Ranade (1987) noted that particle–surface interactions are determined by a wide variety of particle and surface properties, in addition to the particles' shape, size, and distribution. He listed molecular interactions, electrostatic interactions, liquid bridges, double-layer repulsion, and chemical bonds among the influences that conspire to attach a particle to a surface. There is a paucity of data relating these properties or specific molecular traits of the surface to measurements of particle adhesion. The aim of this investigation is to take a more holistic approach; we seek to evaluate removal rates of 3 types of explosives and compare their removal efficiency to that of benchmark ceramic microspheres. Because various types of microspheres are easy to obtain in a range of sizes and their regularity is conducive to modeling, they may be useful surrogates for explosive particles.

Several researchers have used microspheres as surrogates for explosive particles to study noninvasive removal. Fletcher et al. (2008) examined particle removal by air jets from filter and cloth surfaces. Polycarbonate spheres of several sizes

Received 4 April 2011; accepted 24 July 2011.
Funding for this work was provided by the Department of Homeland Security, Science and Technology Directorate, under contract no. HSHQDC-09-C-00131.
Address correspondence to Ryan Keedy, Mechanical Engineering Department, University of Washington, Stevens Way, Box 352600, Seattle, WA 98195, USA. E-mail: rkeedy@uw.edu

were used as surrogates for explosive particles; the smallest microspheres were shown to be significantly more resistant to resuspension than the larger ones. In another removal study, Phares et al. (2000c) simulated explosives by creating spherical monodisperse polystyrene particles laced with trinitrotoluene (TNT). They observed the smaller particles to be more resistant to resuspension; however, once resuspended, they were easier to collect than their larger counterparts.

There are a number of theories on particle detachment. Wang (1990) suggested 3 mechanisms of removal of a single particle: lift-off, sliding, and rolling. Ibrahim et al. (2003) concluded that rolling is likely the primary driver of detachment caused by forced air. However, they cited particle–particle interactions to be a potentially important secondary cause of particle detachment. For the purposes of this paper, we will assume in our analysis and quantitative model that rolling is the dominant mechanism for resuspension. This is a conservative estimate of particle removal, and secondary mechanisms such as particle–particle collisions can be added later.

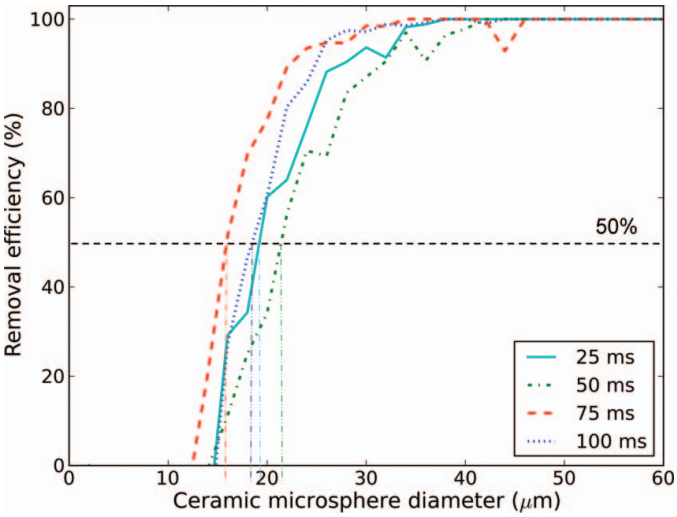

FIG. 2. Ceramic microsphere removal for jet bursts of different durations (2.5 mm nozzle diameter, 276 kPa reservoir pressure, 152 mm standoff distance). (Color figure available online.)

EXPERIMENTAL PROCEDURE

Both ceramic microspheres and explosive particles were interrogated with the same air jet experimental setup. Figure 1 shows a sketch of the experimental layout. The experiments involving the ceramic microspheres were all conducted with a jet issuing from a convergent nozzle of diameter 2.5 mm. However, in order to remove explosive particles at reasonable rates, we found it necessary to increase the nozzle diameter, testing nozzles up to 4.75 mm in diameter. Analyses described later allow for quantitative comparisons to be made across a range of nozzle diameters.

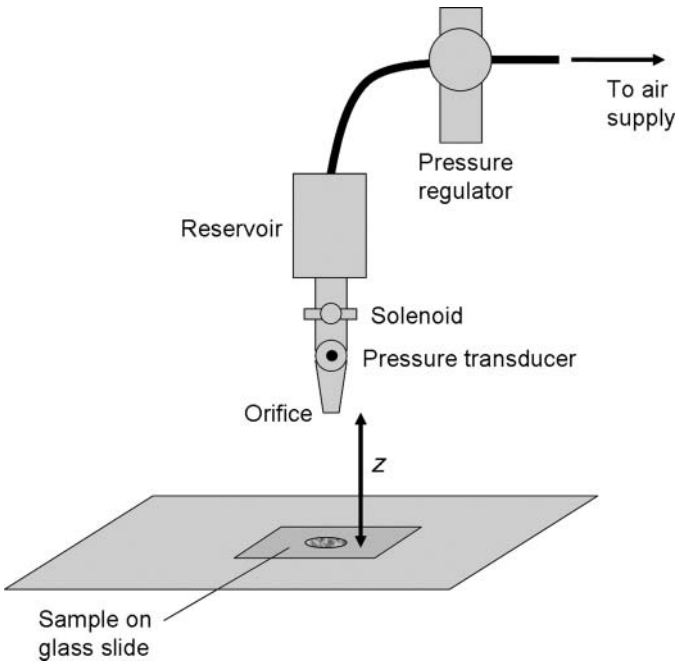

FIG. 1. Diagram of the air jet interrogation experimental setup.

All particles were deposited onto a VWR VistaVision glass slide prior to being interrogated with the air jet. Before deposition, the glass slides were cleaned in an ultrasonic bath and dried. Each prepared glass slide was subjected to a single air pulse. Most tests involved a pulse of approximately 20 ms in duration, although some tests involved longer duration pulses in order to evaluate the effect of pulse duration. Masuda et al. (1994) observed that the duration of the jet, as well as the number of jet pulses used are both known to affect removal rates. All of our experiments, however, used a single jet burst; we did not observe a strong effect due to varying the jet duration from 25 to 100 ms (Figure 2). For the eventual purpose of collecting the removed particles for analysis, a shorter pulse length reduces the dilution of the air to be sampled; therefore, the interrogation of explosive particles was done with air jets of approximately 20 ms duration (significantly smaller pulses being challenging in practice due to solenoid valve limitations). Figure 3 illustrates the resulting volume of air ejected from a 4.5 mm nozzle, as a function of reservoir pressure and pulse duration.

An ASCO Red-Hat II fast-acting solenoid valve controlled the length of the pulse. Supply pressures ranged from 138 to 965 kPa above atmospheric pressure; a reservoir was used upstream of the solenoid to help maintain a constant jet back-pressure for the duration of the pulse. For the values of reservoir pressure tested, the air jet emerges sonically from the nozzle as an underexpanded jet.

Humidity was controlled in the laboratory, maintaining a value of 30%–50%. This is an important consideration, as previous experiments, notably Corn and Stein (1965), have noted that removal efficiency drops significantly at high humidity levels.

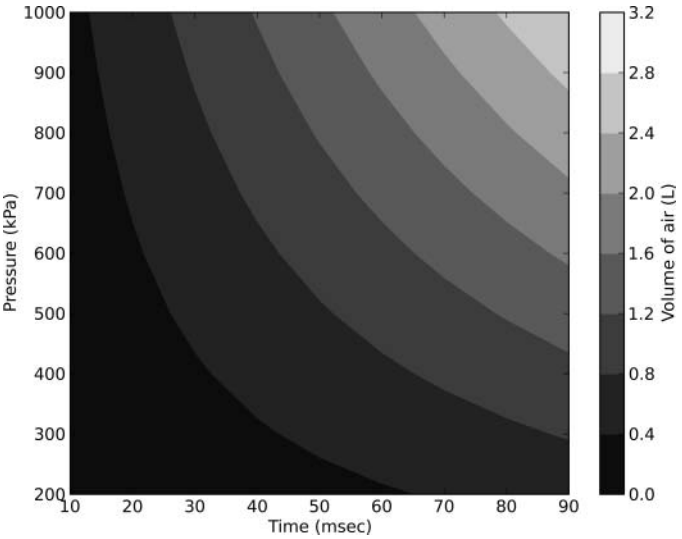

FIG. 3. Volume of air ejected from a 4.5 mm diameter nozzle as a function of reservoir pressure and pulse duration.

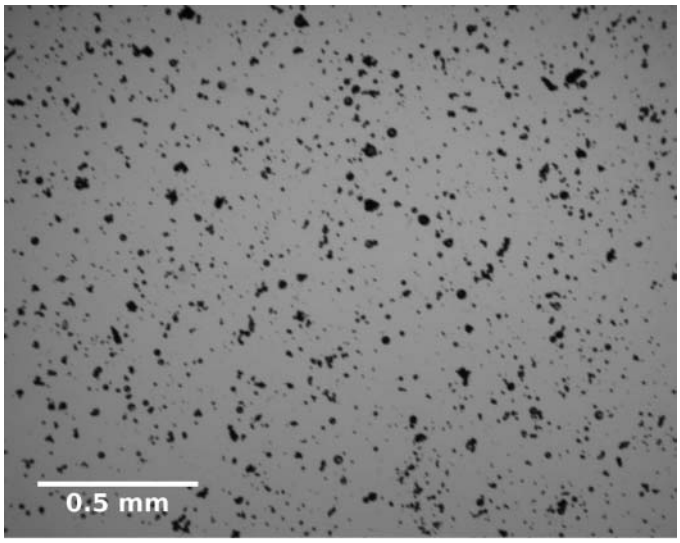

(a) Ceramic microspheres before air jet interrogation.

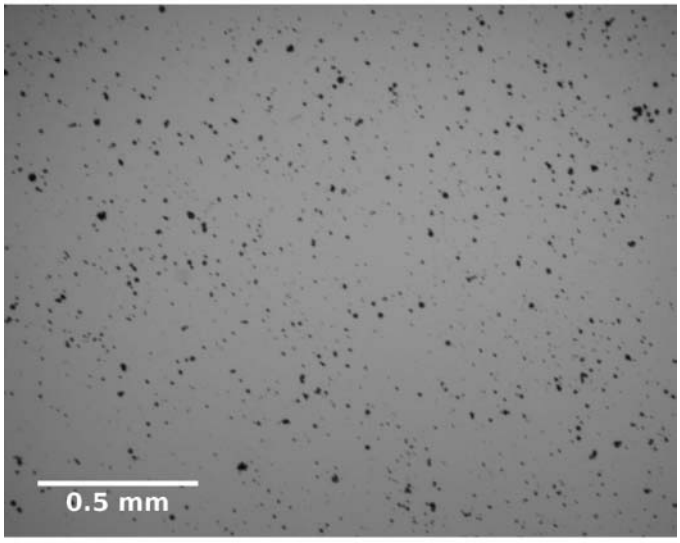

(b) Ceramic microspheres after air jet interrogation.

FIG. 4. Microscope images of ceramic microspheres on glass, both before and after interrogation, by an air jet pulse (2.5 mm diameter nozzle, 207 kPa reservoir pressure, 152 mm standoff distance).

Microsphere Particles

We tested the removal of polydisperse ceramic spheres as a benchmark against which to compare the explosive particles. The test particles were Zeeosphere™ ceramic microspheres G-850 (Zeeospheres Ceramics LLC, Lockport, LA). The mean particle diameter ranges in size between 35 and 60 microns, with a 50-micron mean being reported as typical. Verkouteren (2007) suggests that this is within the range of explosive particle sizes that should be targeted for sampling.

The particles were gravity-deposited directly onto the glass slides (dry transfer via Bytac strip was not used in these experiments) and interrogated at least 24 h later. We expect that this method of deposition yields approximately equivalent removal results to our experiments using explosives (where particles were forcibly applied). Otani et al. (1995) performed experiments showing that a single jet pulse removed particles at comparable rates whether they were deposited by inertial impaction or gravitational settling followed by a waiting period.

For these experiments with ceramic spheres, air supply pressure ranged from 138 to 483 kPa above atmospheric pressure. Standoff distance was varied from 25 to 229 mm ($\hat{z}$ =10–92).

Pictures of the slides were taken under microscopic magnification (Figure 4). ImageJ (NIH, Rasband 1997–2011) was used to analyze the microscopy images before and after interrogation. The percentage of covered area was computed before and after the air jet interrogation. In this manner, removal efficiency was calculated simply as

$$\varepsilon_{rem} = \frac{A_{before} - A_{after}}{A_{before}}. \quad [1]$$

Notice that this surface area removal metric assumes that the mass of explosive is deposited in a single layer with uniform thickness. This is an approximation that by being used consistently across the experiments described in this study allows for quantitative comparisons to be made.

In addition to making an area measurement, image processing was also used to determine the size distribution of the particles present. Because the ceramic particles were known to be spheres, the number of each size of particles could be determined from the images. The particle size that experienced 50% removal was determined by analysis of various particle size bins both before and after interrogation by the air jet. The ratio of the particle count before and after removal was converted to a percentage removal for each particle diameter range. Plotting the data as a function of diameter, we expect the curves of removal (one curve for each experiment) to cross the 50% removal level at the relevant particle diameter.

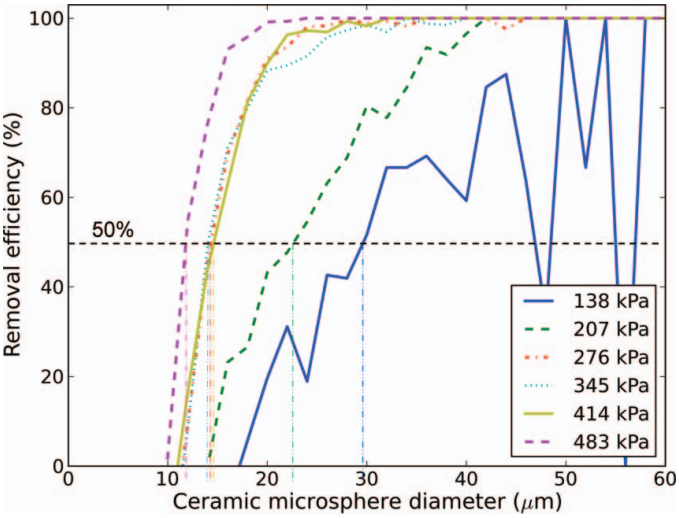

FIG. 5. Ceramic microsphere removal for jet bursts with varying reservoir pressures (2.5 mm diameter nozzle, 152 mm standoff distance). (Color figure available online.)

One drawback of this approach is that if multiple particles are deposited adjacent to each other, the software may incorrectly account for them as a single large particle instead of several small particles. In addition, the number of particles necessary for reliable analysis may challenge the approximation we are making that particle-to-particle interactions are not a main driver of particle removal.

Figure 5 shows removal efficiency data as a function of particle diameter for several experiments by varying the supply pressure. The data tend to become noisier at larger particle diameters because they occur with less frequency than the smaller particles; the relatively small number of particles before interrogation leads to removal rates calculated using relatively small sample sizes. Despite challenges with the sample sizes, there is a clear trend that particle removal efficiency depends strongly on the jet reservoir pressure.

Explosive Particles

Chamberlain (2002) has outlined a procedure for preparing explosives for sampling, which we used in these experiments. C-4, TNT, and research development explosive (RDX; cyclotrimethylenetrinitramine) were obtained as solutions in acetonitrile at known concentrations. In order to prepare a sample, a volume of the solution, proportional to the mass of explosive desired (typically 5 μg), was deposited onto a 1" $\times$ 1" Bytac coupon. A drying chamber was used to speed up evaporation of the acetonitrile, resulting in the formation of crystal structures of trace explosive. The relatively low volatility of the explosive (O[0.01 Pa] versus O[10 Pa] for acetonitrile) allowed us to predict that the mass of the explosive was conserved during the drying process.

The explosives were then applied to glass slides by rubbing the coupon back and forth several times against the surface. This transfer was performed (as opposed to directly depositing the explosive solution onto the slide) in order to ensure repeatability and to remain consistent with the procedure outlines by Chamberlain (2002). Had the explosive particles been wet-deposited onto the glass surface, work from Bhattacharya and Mittal (1978) suggests that the particles would adhere much more strongly than in these experiments that use dry deposition. Furthermore, the transfer allowed the homogenous, condensed explosive to be broken up into smaller particles upon transfer. TNT was particularly prone to form a single solid structure upon evaporation of the acetone; applying the transfer technique described by Chamberlain allowed it to break up into many smaller particles (Figure 6).

The glass slides were interrogated shortly (less than 5 min) after application. The experimental setup for trace explosives removal was identical to the one used for ceramic spheres, as shown in Figure 1. The pressure regulator was varied to establish

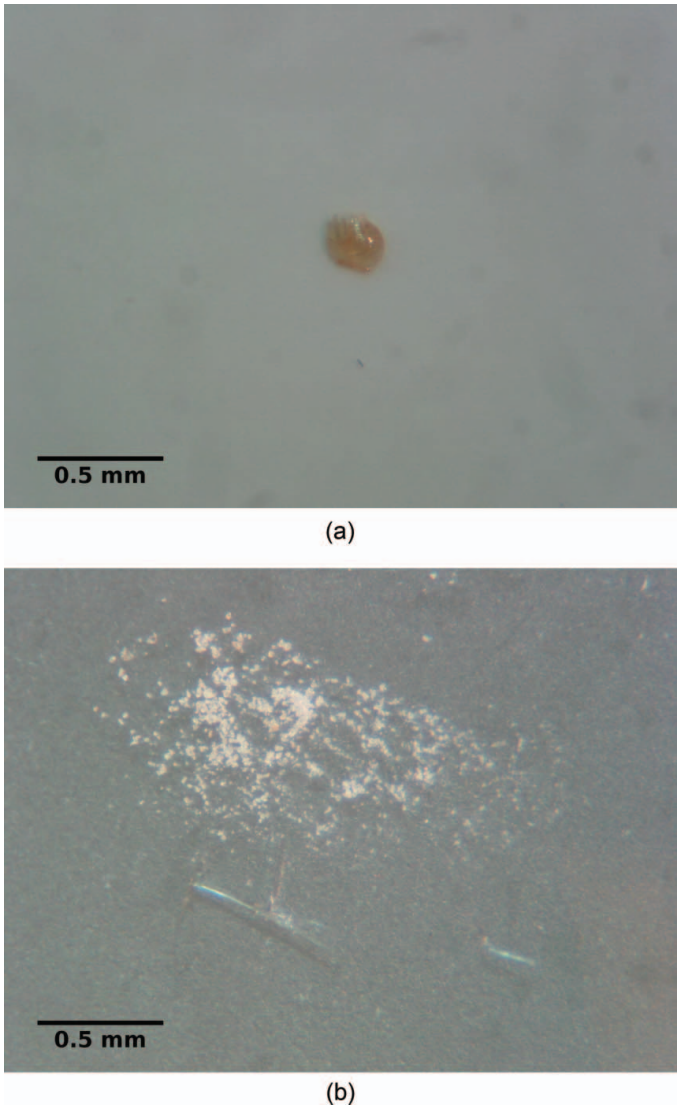

FIG. 6. Microscopic images of TNT before and after transfer. (a) Solid TNT nugget (5 μg) resulting from desiccation. (b) TNT particles after transfer. (Color figure available online.)

the supply pressure between 172 and 965 kPa. We measured the pressure and pulse duration just upstream of the nozzle using an SSI MediaSensor P51 pressure transducer. The nozzle diameters tested were 2.5, 4.0, 4.5, and 4.75 mm. Vertical standoff from the nozzle to the glass slide spanned from 25 to 152 mm.

Because the explosive particles' shape and size distribution are irregular, options for evaluating removal are limited. The masses involved are too small to be weighed reliably ($\leq$5 μg). Also, individual particles sometimes cannot be optically resolved due to their proximity to each other. Even if the individual particles could be resolved, their irregular shapes would make the determination of their volume (and therefore their mass) subjective. Instead, we chose to measure the area covered by particles before and after interrogation, and compare them to determine removal efficiency (neglecting thickness of deposition).

Photographs were taken while examining the slides under a microscope both before and after the test (Figure 7). ImageJ was used to analyze the images, calculating the area covered before and after the air jet interrogation, and removal efficiency was computed as defined in Equation (1).

In addition, particle size analysis was conducted in the same manner as it was done for the ceramic microspheres, though the uncertainty is higher due to the inability to identify internal boundaries of large explosive deposits. Figure 8 compares the results of histograms compiled from microscope images of the various particle types. Note that the 3 types of explosives exhibit high similarity in particle size distributions, all of them having a wider distribution of particle sizes than the ceramic microspheres. However, Table 1 shows that for various particle distribution metrics, the 4 particles are quantitatively similar.

REMOVAL MODELING

In order to remove a spherical particle from the surface by rolling, Phares et al. (2000a) proposed that the tangential drag force, applied at the particle center, must satisfy

$$F_{drag} = \frac{2aF_a}{d_p}, \qquad [2]$$

where F_a is the attachment force and a is the contact radius. Rimai et al. (1990) showed that a is proportional to the square root of the particle diameter,

$$a \propto \sqrt{d_p} \qquad [3]$$

TABLE 1
Particle size distribution properties

	Zeeospheres™	TNT	C-4	RDX
Median d_p (μm)	16	12	13	12
D_{10} (μm)	18	16	18	15
σ_d (μm)	9	13	16	11
D_{20} (μm)	20	21	24	18

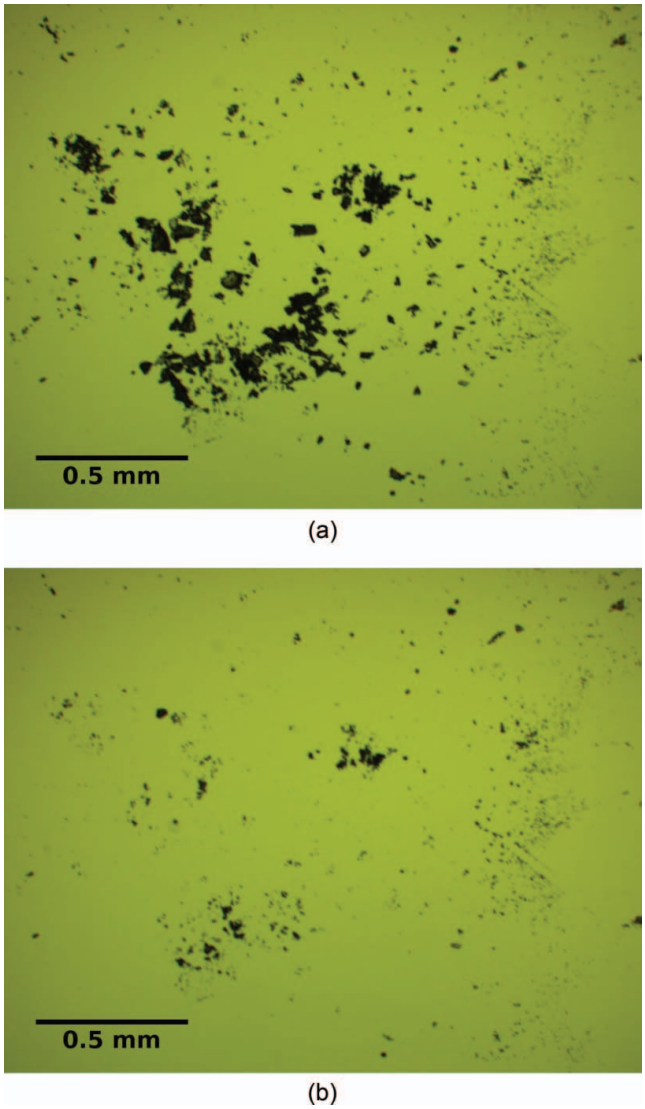

FIG. 7. Microscopic images of TNT on glass, both before and after interrogation, by an air jet pulse (4.75 mm diameter nozzle, 655 kPa reservoir pressure, 47 mm standoff distance). (a) TNT before air jet interrogation. (b) TNT after air jet interrogation. (Color figure available online.)

and that the attachment force is proportional to a^2, which implies that it is proportional to d_p:

$$F_a \propto d_p. \qquad [4]$$

That leaves the drag force to be determined. Phares also made use of the Galileo number ($Ga = C_D Re_p^2$), from which we can find a relationship between F_{drag} and d_p,

$$F_{drag} = \frac{\pi \mu^2 C_D Re_p^2}{8\rho} = \frac{1}{8}\pi\rho C_D d_p^2 V^2 \qquad [5]$$

$$F_{drag} \propto d_p^2 V^2 \qquad [6]$$

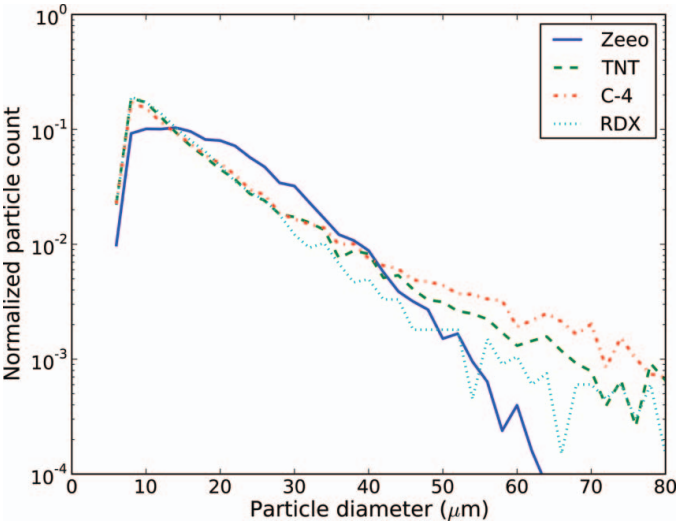

FIG. 8. Histograms of particle size for the 4 types of particles in our study. (Color figure available online.)

assuming that C_D and ρ are constant. With the particle residing in the viscous sublayer, for a given flow intensity, we expect the velocity at the particle's centerline to be proportional to its height, d_p, and to the shear stress, τ, ($V \propto d_p\tau$) leading to

$$F_{drag} \propto d_p^4\tau^2. \quad [7]$$

Thus, the condition for removal, Equation (2), can be rewritten as

$$d_p^{7/2} = \frac{C_1}{\tau^2}, \quad [8]$$

where C_1 is a product of constants (and thus, a constant itself). Alternatively, and perhaps more usefully, we can determine the critical shear stress required as it relates to the particle diameter:

$$\tau = \frac{C_2}{d_p^{7/4}}. \quad [9]$$

The shear stress at the surface can be estimated on the basis of analytical derivations presented in the literature. For a self-similar free jet, Phares et al. (2000b) derived a relationship indicating that surface shear is proportional to $V_{CL}^{3/2}$. Consolidating the constants to C_3, we can find a criterion for the removal of an individual particle using air jet velocity instead of shear stress:

$$V_{CL}^{3/2}d_p^{7/4} = C_3. \quad [10]$$

Finally, Birch et al. (1987) established that in the developed region, $V_{CL}^{-1} \propto \zeta$, yielding the following criterion:

$$\zeta = Kd_p^{7/6}. \quad [11]$$

The value ζ is a nondimensional downstream distance that incorporates the effect of the jet reservoir pressure, standoff distance, and nozzle diameter. Due to the different experimental conditions used, ζ is an important nondimensional variable that enables the comparison of different results across experiments. Birch determined the nondimensionalized axial downstream distance of an underexpanded air jet by defining an effective jet diameter (d_e) and virtual origin (z_0) that are functions of the jet reservoir pressure. Plotted against this nondimensional distance, the inverse of the jet velocity along the centerline collapses to a single linear profile (outside of the development region).

The nondimensional distance, ζ, is defined as

$$\zeta = \frac{z^*}{d_e}, \quad [12]$$

where d_e is the effective diameter and z^* is the adjusted downstream distance, accounting for the virtual origin. Specifically,

$$d_e = d\sqrt{\frac{P_0}{P_a}\left(\frac{2}{\gamma+1}\right)^{\frac{1}{\gamma-1}}\frac{V_0}{V_e}}, \quad [13]$$

where P_0 is the jet reservoir pressure (absolute), P_a is the ambient pressure, γ is the heat capacity ratio, and

$$V_e = \frac{V_0}{\gamma}\left[1+\gamma-\frac{P_a}{P_0}\left(\frac{2}{\gamma+1}\right)^{-\frac{\gamma}{\gamma-1}}\right]. \quad [14]$$

The coordinate for downstream distance, z^*, is defined simply as $z^* = z - z_0$ where z_0 is the virtual origin. Birch provides an empirical relationship for z_0 versus reservoir pressure. Therefore, ζ is a function of z, d, and jet reservoir pressure P_0. Figure 9 provides an illustration of the various geometrical parameters used.

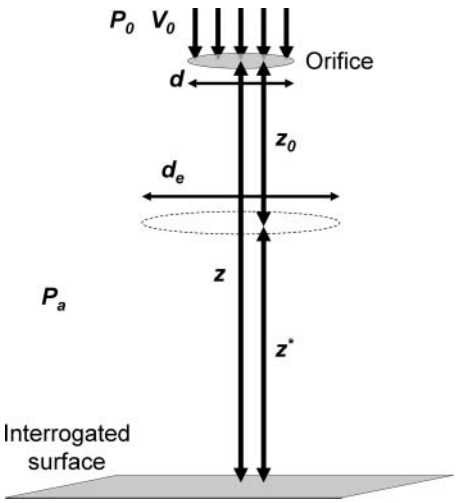

FIG. 9. Diagram of dimensions used for analysis.

EXPERIMENTAL DATA

Microsphere Particles

Considering Equation (11), K is best determined experimentally because it incorporates a number of undetermined constants. Taking into account the variability of ceramic sphere diameters, it is best to use a statistical interpretation of the deterministic model. Instead of focusing on the removal of a single particle, we will define the constant K that results in 50% removal of particles of a given diameter.

We first plot the data collected from the ceramic microsphere removal tests over a range of supply pressures and standoff distances. Figure 10 plots the ceramic particle diameter exhibiting 50% removal rates as a function of ζ. Because ζ is a function of the jet reservoir pressure and standoff distance (and nozzle diameter), this allows us to overlay the results from many different experiments. A best-fit least-squares curve is also plotted, based on Equation (11), where K was determined to be 1.35 μm$^{6/7}$. The data for removal of ceramic microspheres under a wide variety of experimental conditions are reasonably well described by the theoretical model.

Explosive Particles

After experimentally determining the value of ζ corresponding to 50% removal of a particular explosive, an appropriately sized ceramic microsphere surrogate can be selected using Equation (11). We expect such a monodisperse surrogate to experience 50% removal under similar conditions as the explosive. However, the explosives tested all exhibited 50% removal at negative values of ζ (upstream of the virtual origin z_0). Being upstream of the self-similar region of the jet, the relationships outlined by Birch are not quantitatively accurate, and Equation (11) does not adequately describe the relationship between

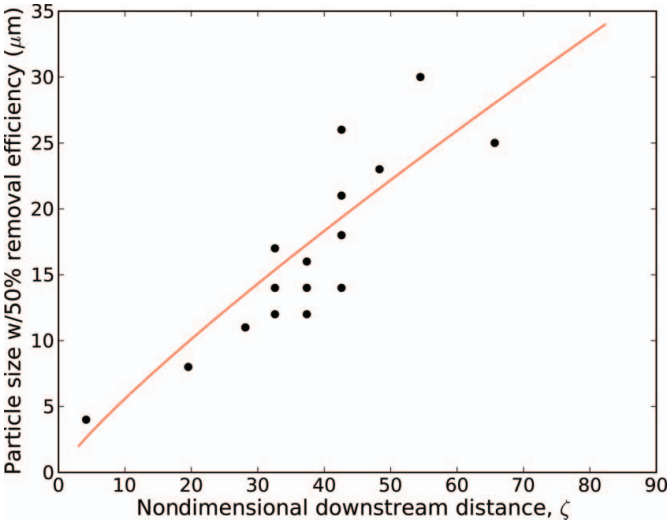

FIG. 10. Plot of experimental data for ceramic microsphere particle diameter experiencing 50% removal at various ζ; data are fit with the curve from Equation (11), $K = 1.35\,\mu\text{m}^{6/7}$. (Color figure available online.)

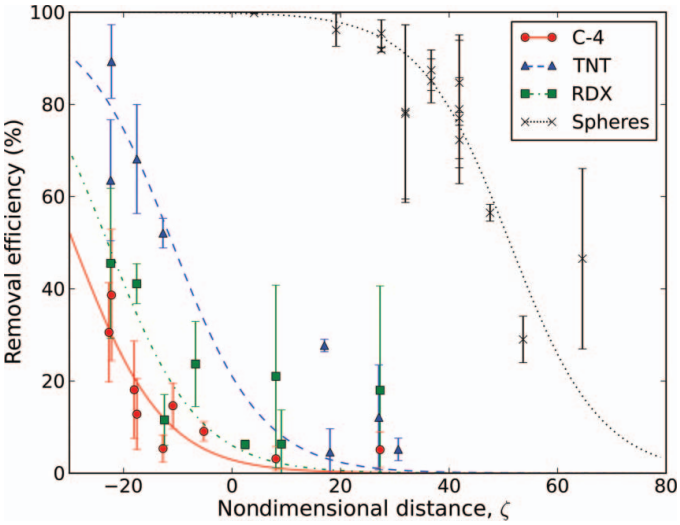

FIG. 11. Plot of removal versus ζ for 3 explosives and ceramic microspheres [experimental results as points; curve fits from Equation (15) as lines]. (Color figure available online.)

downstream distance and removal. While we can no longer assume that removal will depend on ζ according to Equation (11), it is reasonable to expect that there will still be a similar qualitative dependency.

Quantifying explosive particle removal as a function of diameter was difficult due to the variability in explosive particle shapes. Despite the fact that the deposition procedure was consistently followed, the explosive material was often deposited in irregular patterns with ill-defined internal boundaries. Because of the lack of certainty in size and shape of the particles, we chose instead to measure the explosive area removed against ζ. Figure 11 shows results for the 3 explosives tested as well as the ceramic particle tests. Although we cannot quantify the maximum shear stress as a function of negative values of ζ, it is possible to report the value ζ_{50} that elicits 50% removal. In an effort to represent the data in a straightforward manner with a clearly defined demarcation for 50% removal, we fitted each set of particle removal data with a sigmoid curve. Each curve had the following form:

$$\varepsilon_{rem}(\zeta) = \frac{1}{1 + e^{0.12(\zeta - \zeta_{50})}}, \qquad [15]$$

where ζ is the independent variable and ζ_{50} uniquely defines the horizontal location of each curve. The coefficient 0.12 was chosen to best match the behavior of all particle types. By applying a least squares fit criterion, ζ_{50} can be determined for each type of particle. It can be reasonably expected that under different conditions, the values of ζ_{50} may change, but we expect relative removal rates of the explosives to remain unchanged as long as the mechanism of particle removal from the surface remains the same.

It appears that the fit of the data may be worse at higher values of ζ. We observed that occasionally, the explosive transfer

was not efficient in breaking up some of the larger particles. These large particles were removed at relatively high values of ζ, resulting in disproportionate coverage reduction and a high value of ε_{rem}.

C-4 proved the most difficult to remove, with a ζ_{50} value of -29. RDX was slightly easier at -23, and TNT was the easiest of the 3 explosives to remove at $\zeta_{50} = 11$. The ceramic microspheres, on the contrary, were removed at a standoff distance of $\zeta_{50} = 51$.

SUMMARY

Explosive particles were found to be much more difficult to remove than their ceramic counterparts, despite the apparent similarity in particle size distributions. In order to achieve 50% removal, it was necessary to subject the explosives to the underexpanded, undeveloped region of the jet. This makes it difficult to quantify the shear stress needed for removal, but the nondimensional downstream distance, ζ, may be used instead.

The removal rate was observed to depend strongly on the type of explosive being examined, as well as being a function of ζ. There are several factors that could lead to different removal rates for different explosives. While the particle size distributions were similar among the explosives and ceramic microspheres, we have little information regarding the shapes of the explosive particles. It is reasonable to assume that they are not spherical, but we cannot speculate as to whether the different explosive particles have characteristically dissimilar shapes, which would potentially result in different removal rates.

It is perhaps most natural to attribute the differences in removal rate to the chemistry of the particle and substrate involved. Since we use a glass substrate in all of our experiments, the adhesive force of each explosive can be impartially evaluated; other substrates may prove to either enhance or diminish the removal trends we observed.

The differences in ζ_{50} values indicate that TNT particles were easier to remove than RDX; C-4 particles appeared to require the highest shear stress to be resuspended. For example, given a 4.75 mm nozzle diameter, and a modest standoff of $\hat{z} = 20$, our results from Figure 11 indicate that 50% removal of TNT particles would require 790 kPa of supply pressure, 50% removal of RDX would require 1100 kPa, and 50% removal of C-4 would require 1300 kPa (the latter 2 pressures were never reached in this study). The ceramic microspheres we tested, on the contrary, should require less than 150 kPa for 50% removal. It is unclear, due to the limitations of our shear stress analysis, exactly what diameter a ceramic microsphere would need in order to behave as a surrogate for each explosive, but the typical diameter would need to be significantly smaller than 10 μm.

NOMENCLATURE

d_p	Particle diameter
z	Nozzle standoff distance
z_0	Downstream distance of virtual origin
z^*	Virtual downstream distance ($z - z_0$)
d	Nozzle diameter
P_0	Reservoir (supply) pressure for jet
V_{CL}	Center-line jet velocity
V_0	Jet exit velocity, Equation (14)
d_e	Effective nozzle diameter, Equation (13)
V_e	Effective jet exit velocity, Equation (14)
ε_{rem}	Particle removal efficiency (by area)
$\hat{z}$	Dimensionless downstream distance (z/d)
ζ	Effective virtual downstream distance, Equation (12)
ζ_{50}	Value of ζ corresponding to 50% removal

REFERENCES

Bender, E., Hogan, A., Leggett, D., Miskolczy, G., and MacDonald, S. (1992). Surface Contamination by TNT. *J. Forensic. Sci.,* 37:1673–1678.

Bhattacharya, S., and Mittal, K. (1978). Mechanics of Removing Glass Particulates from a Solid Surface. *Surf. Technol.*, 7(5):413–425.

Birch, A., Hughes, D., and Swaffield, F. (1987). Velocity Decay of High Pressure Jets. *Combust. Sci. Technol.*, 52:161–171.

Chamberlain, R. (2002). Dry Transfer Method for the Preparation of Explosives Test Samples. U.S. Patent No. 6,470,730.

Corn, M., and Stein, F. (1965). Re-entrainment of Particles from a Plane Surface. *Am. Ind. Hyg. Assoc. J.*, 26(4):325–336.

Davidson, W., and Stott, W. (2002). Vapor and Particle Sampling in the Detection of Terrorist Explosives, in *Proceedings of 50th ASMS Conference on Mass Spectrometry and Allied Topics*, pp. 697–698.

Fletcher, R., Briggs, N., and Ferguson, E. (2008). Measurements of Air Jet Removal Effciencies of Spherical Particles from Cloth and Planar Surfaces. *Aerosol Sci. Tech.*, 42(12):1052–1061.

Ibrahim, A., Dunn, P., and Brach, R. (2003). Microparticle Detachment from Surfaces Exposed to Turbulent Air Flow: Controlled Experiments and Modeling. *J. Aerosol Sci.*, 34:765–782.

Masuda, H., Gotoh, K., Fukada, H., and Banba, Y. (1994). The Removal of Particles from Flat Surfaces Using a High-Speed Air Jet. *Adv. Powder Technol.*, 5(2):205–217.

National Research Council (2004). *Committee on the Review of Existing and Potential Standoff Explosives Detection Techniques*. National Research Council, The National Academies Press, Washington, DC.

Otani, Y., Namiki, N., and Emi, H. (1995). Removal of Fine Particles from Smooth Flat Surfaces by Consecutive Pulse Air Jets. *Aerosol Sci. Tech.*, 23(4):665–673.

Phares, D., Smedley, G., and Flagan, R. (2000a). Effect of Particle Size and Material Properties on Aerodynamic Resuspension from Surfaces. *J. Aerosol Sci.*, 31(11):1335–1353.

Phares, D., Smedley, G., and Flagan, R. (2000b). The Wall Shear Stress Produced by the Normal Impingement of a Jet on a Flat Surface. *J. Fluid Mech.*, 418:351–375.

Phares, D. J., Holt, J. K., Smedley, G. T., and Flagan, R. C. (2000c). Method for Characterization of Adhesion Properties of Trace Explosives in Fingerprints and Fingerprint Simulations. *J. Forensic. Sci.*, 45(4):774–784.

Ranade, M. (1987). Adhesion and Removal of Fine Particles on Surfaces. *Aerosol Sci. Tech.*, 7(2):161–176.

Rasband, W. (1997–2011). *ImageJ*. U.S. National Institutes of Health, Bethesda, MD. Available online at: http://imagej.nih.gov/ij/,.1997-2011.

Rimai, D., DeMejo, L., and Bowen, R. (1990). Surface-Force-Induced Deformations of Monodisperse Polystyrene Spheres on Planar Silicon Substrates. *J. Appl. Phys.*, 68(12):6234–6240.

Verkouteren, J. (2007). Particle Characteristics of Trace High Explosives: RDX and PETN. *J. Forensic. Sci.*, 52(2):335–340.

Wang, H.-C. (1990). Effects of Inceptive Motion on Particle Detachment from Surfaces. *Aerosol Sci. Tech.*, 13(3):386–393.